Tectonophysics 497 (2011) 1–14

Contents lists available at ScienceDirect

Tectonophysics

journal homepage: www.elsevier.com/locate/tecto

Left-lateral active deformation along the Mosha–North Tehran fault system (Iran): Morphotectonics and paleoseismological investigations

Shahryar Solaymani Azad [a,b,*], Jean-François Ritz [a], Mohammad Reza Abbassi [c]

[a] Université Montpellier 2, Laboratoire Géosciences Montpellier, UMR CNRS 5243, France
[b] Seismotectonic Group, Geological Survey of Iran (GSI), Azadi Sq., Meraj Ave., 13185-1494, Tehran, Iran
[c] International Institute of Earthquake Engineering and Seismology (IIEES), North Dibaji, West Arghavan, # 21, Tehran, Iran

ARTICLE INFO

Article history:
Received 3 October 2009
Received in revised form 14 August 2010
Accepted 12 September 2010
Available online 27 September 2010

Keywords:
Iran
Central Alborz
Mosha fault
North Tehran fault
Active fault
Morphotectonics

ABSTRACT

The Mosha and North Tehran faults correspond to the nearest seismic sources for the northern part of the Tehran megacity. The present-day structural relationships and the kinematics of these two faults, especially at their junction in Lavasanat region, is still a matter of debate. In this paper, we present the results of a morphotectonic analysis (aerial photos and field investigations) within the central part of the Mosha and eastern part of the North Tehran faults between the Mosha valley and Tehran City. Our investigations show that, generally, the traces of activity do not follow the older traces corresponding to previous long-term dip–slip thrusting movements. The recent faulting mainly occurs on new traces trending E–W to ENE–WSW affecting Quaternary features (streams, ridges, risers, and young glacial markers) and cutting straight through the topography. Often defining en-echelon patterns (right- and left-stepping), these new traces correspond to steep faults with either north- or south-dipping directions, along which clear evidences for left-lateral strike–slip motion are found. At their junction zone, the two sinistral faults display a left-stepping en-echelon pattern defining a positive flower structure system clearly visible near Ira village. Further west, the left-lateral strike–slip motion is transferred along the ENE–WSW trending Niavaran fault and other faults. The cumulative offsets associated with this left-lateral deformation is small compared with the topography associated with the previous Late Tertiary thrusting motion, showing that it corresponds to a recent change of kinematics.

1. Introduction

The Mosha and North Tehran faults correspond to two major structures in the southern border of the Central Alborz, the active mountain range surrounding the southern margin of the South Caspian basin (e.g. Berberian, 1983; Jackson et al., 2002; Allen et al., 2003a). These faults are located at the immediate vicinity of the highly-populated region of Tehran, where more than 15 million people are living (Fig. 1). The Mosha and North Tehran faults represent an important seismic hazard for the Iranian capital considering the historical seismicity recorded in the area (e.g. Ambraseys and Melville, 1982; Berberian and Yeats, 1999) and the active tectonics features observed along them (e.g. Berberian et al., 1985; Trifonov et al., 1996; Ritz et al., 2003; Solaymani et al., 2003; Nazari, 2006; Ritz et al., 2006).

The present kinematics of these two faults, especially at their junction is still a matter of debate. Geologically, at a regional scale, the Mosha and North Tehran faults are mapped as north-dipping thrust faults, along which Jurassic and older formations (for the Mosha fault) and Eocene formations (for the North Tehran fault) are thrusting over Eocene rocks and Pliocene–Quaternary deposits, respectively (e.g. Geological survey of Iran, 1993). As concerns their present-day kinematics, the two faults are classically described as mainly thrusts (e.g. Tchalenko, 1975; Berberian, 1976; Berberian and Yeats, 1999, 2001), that join together in the Lavasanat region (e.g. Tchalenko, 1975; Berberian et al., 1985; Bachmanov et al., 2004). Lavasanat is the regional name of the area situated in the junction zone of the two faults (see Fig. 1).

However, recent active tectonics studies describe clear active left-lateral strike–slip deformation along the WNW–ESE trending eastern Mosha fault (e.g. Allen et al., 2003b; Ritz et al., 2003; Solaymani et al., 2003; Ashtari et al., 2005; Ritz et al., 2006). Recent left-lateral strike–slip deformation as a component of a main transpressional deformation is also described along the North Tehran fault, within its eastern ENE–WSW trending section (e.g. Hessami et al., 2003; Bachmanov et al., 2004; Landgraf et al., 2009).

The present geometry, spatial extent and kinematics of the two active faults in their junction zone (Lavasanat region, see Fig. 1) remain in question. In this paper, by means of a morphotectonic study using aerial photo interpretations and field investigations, we analyze the present-day structural relationships and kinematics between the

* Corresponding author. International Institute of Earthquake Engineering and Seismology (IIEES), North Dibaji, West Arghavan, # 26, Tehran, Iran. Tel.: +982164592468.
E-mail addresses: shahryar_solaymani@yahoo.com, shahryar.solaymani@gmail.com (S. Solaymani Azad).

0040-1951/$ – see front matter © 2010 Elsevier B.V. All rights reserved.
doi:10.1016/j.tecto.2010.09.013

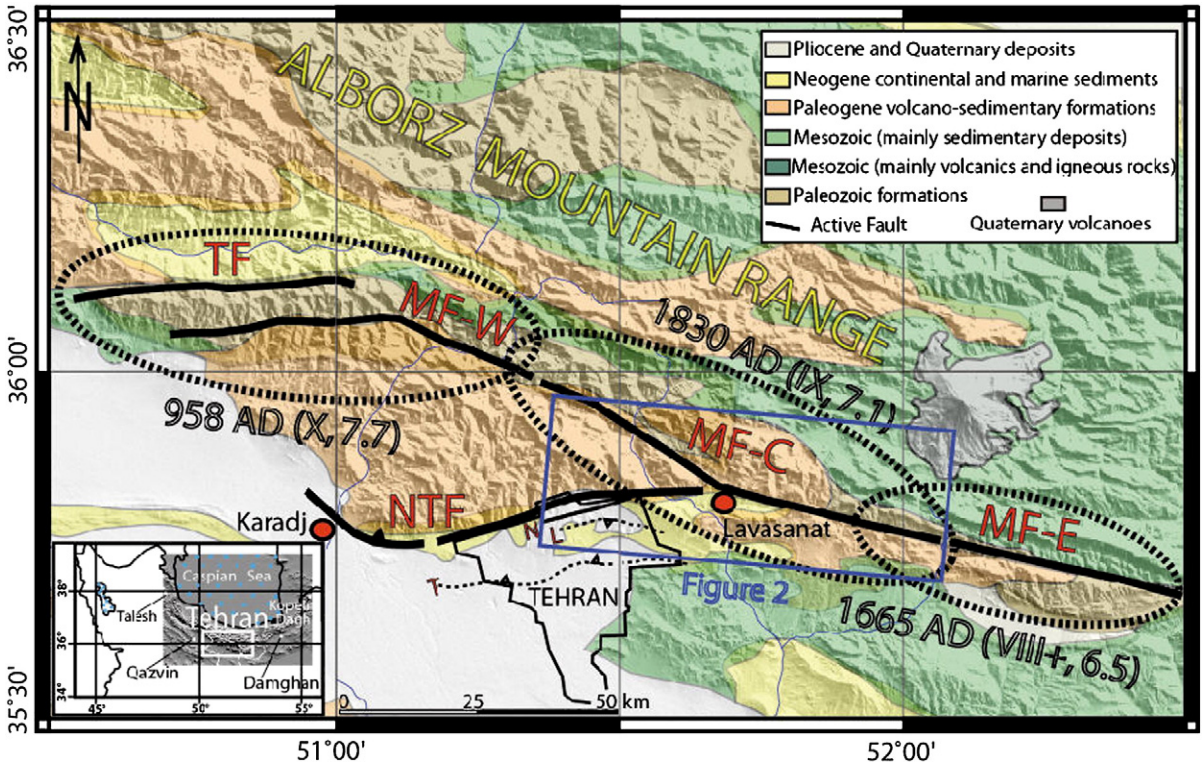

Fig. 1. Sketch map of the Mosha and the North Tehran faults in the southern border of the Central Alborz mountain range overlaid on simplified geological map and SRTM digital elevation model (http/:edcsgs9.cr.usgs.gov/pub/data/srtm/), and the three damaging historical earthquakes (black dashed ellipsoids) classically attributed to this area. NTF: North Tehran fault, TF: Taleghan fault, MF-W: Western Mosha fault, MF-E: Eastern Mosha fault, MF-C: Central Mosha fault. N: Niavaran fault; L: Lavizan fault; and T: Tarasht fault. The blue frame indicates our study area within the meizoseismal zone of the 1830 AD event. The meizoseismal areas are from Berberian and Yeats (1999) and their evaluated intensities and magnitudes are from Ambraseys and Melville (1982). L and T fault traces are after Abbassi and Farbod (2009).

central part of the Mosha fault and the eastern part of the North Tehran fault.

2. Tectonic setting

The Alborz mountain range corresponds to an active mountain belt surrounding the South Caspian oceanic domain (e.g. Berberian, 1983; Jackson et al., 2002; Allen et al., 2003a) and can be described as the northern part of the Alpine–Himalayan orogenic belt in Western Asia (e.g. Stöcklin, 1974). This sinuous range extends over 900 km and can be subdivided in three major parts. The longer one, the Central Alborz, extends for about 600 km along the southern side of the Caspian Sea from Qazvin (49°00′E, 36°15′N) to Damghan (54°30′E, 36°15′N) (see regional map enclosed in Fig. 1). We define the Western Alborz as the portion of the mountain range setting from Qazvin to the Talesh, and the Eastern Alborz as the part situated between Damghan and the Kopeh Dagh mountain range. The Central Alborz formed a ~100 km wide belt, characterized by range-parallel folds and faults showing opposite vergences (e.g. Stöcklin, 1968, 1974; Berberian, 1983; Jackson et al., 2002; Allen et al., 2003b). Between longitudes 50°E to 54°E, a wide "V" shape structure characterizes its general form, with folds and faults trending NW–SE in the western part and NE–SW in the eastern part. The geological and tectonics history of Alborz is complex with several orogen episodes (e.g. Alavi, 1996) separated by extensional phases (e.g. Berberian, 1983; Zanchi et al., 2006). This range developed due to closure of the Paleothetys ocean and was

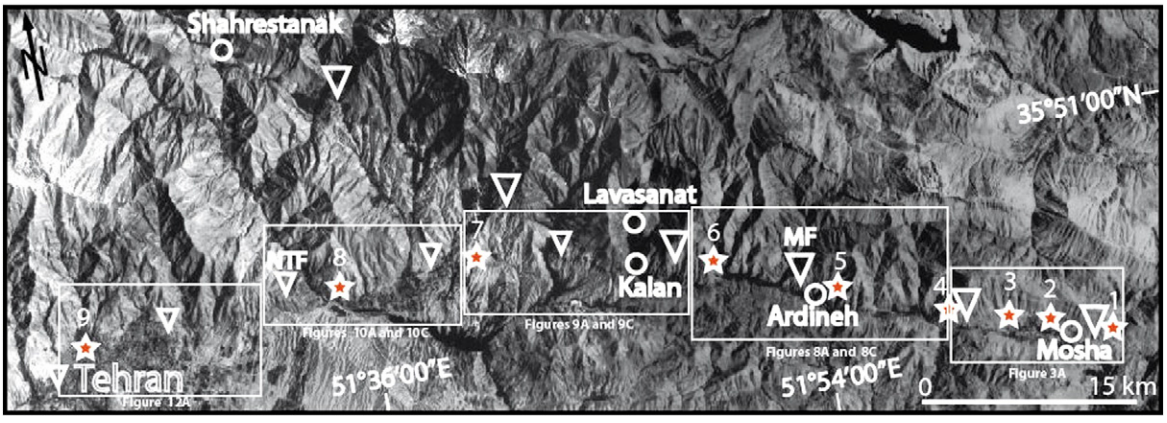

Fig. 2. Cosmos satellite image (pixel size 10 m) of the region situated in the NE of Tehran City. The triangles point out the traces of the central part of the Mosha fault (MF) and the eastern part of the North Tehran fault (NTF). The white frames show the situation of aerial photographs studied from east to west. The stars indicate the 9 sites studied in details.

affected by Kimmerian and Alpine orogenesis (Stöcklin, 1974), with the major orogenic event occurring in the Oligocene (Stöcklin, 1968; Berberian and King, 1981). Estimates of total shortening across Central Alborz vary from 35–38 km (Nazari, 2006) to 53 km (Guest et al., 2006). Most of it (25–30 km) occurred since Neogene (Allen et al., 2003b; Nazari, 2006).

Neotectonics and seismological studies show that the present-day deformation in Alborz is partitioned along range-parallel thrusts and left-lateral strike–slip faults (e.g. Jackson et al., 2002; Allen et al., 2003a; Ritz et al., 2006; Nazari, 2006; Hollingsworth, 2007). Evidences of left-lateral deformation are documented by focal mechanisms of earthquakes within the western part of Central Alborz along the Rudbar–Manjil fault zone (e.g. Jackson et al., 2002; Tatar and Hatzfeld, 2009) or in the eastern part of Central Alborz along the Mosha fault (e.g. Hedayati et al., 1976; Ashtari et al, 2005), and by fault kinematics deduced from morphotectonic studies along several range-parallel faults such as the Mosha fault (e.g. Trifonov et al., 1996; Ritz et al., 2003; Solaymani et al., 2003; Allen et al., 2003b; Hessami et al., 2003; Bachmanov et al., 2004) or the Taleghan fault (Nazari, 2006; Nazari et al., 2009).

According to Jackson et al. (2002), this active strain partitioning is a result of oblique compression due to the combination of the Arabia–Eurasia northwards convergence and the north–westward motion of the South Caspian basin with respect to stable Eurasia. A recent GPS study quantified the partitioning at the scale of the whole range: the N–S shortening across the range occurs at 5 ± 2 mm/year, while the left-lateral shear across it occurs at a rate of 4 ± 2 mm/year (Vernant et al., 2004; Djamour, 2004). A recent update of the geodetic data gives shortening rates varying from 0 to 5.5 mm/year (most of it being in the north–western part) and a left-lateral shearing across the range from 1.5 to 6.0 mm/year (most of it setting in the south–eastern part) within the Central Alborz (Djamour et al., 2008).

To explain this present-day tectonic setting, authors (e.g. Axen et al., 2001; Jackson et al., 2002; Allen et al., 2003a; Ritz et al., 2006; Ballato et al., 2008; Hollingsworth et al., 2008) invoke a regional change in kinematic during the Neogene. First, the Alborz started to shorten under a North–South compression leading to the formation of ~E–W trending parallel folds and thrusts structures. The recent study of Ballato et al., 2008 reveals that the southward propagation of thrusting and folding within the southern Alborz occurred beyond ~6.2 Ma, which is the age of the Hezardarreh formation corresponding to the conglomerates found at the base of the foreland basin in the Tehran region. During this stage, the South Caspian basin would have been fixed with respect to Eurasia; then, during a second stage, the South Caspian basin started to move towards the north–west with respect to Eurasia (e.g. Jackson et al., 2002). The timing of the onset of the north–west motion is still in debate and varies between 10 Ma (Hollingsworth et al., 2008), ~5 Ma (Axen et al., 2001; Allen et al., 2003a) and 1.5 Ma (Ritz et al., 2006). Recently, Ritz (2009) suggested that the recent motion of the South Caspian basin occurred in two stages: during a first stage at the end of the Miocene, the basin started to subduct to the north beneath the Apsheron Sill (located in northern limit of the South Caspian basin), and then a westward component of motion has been added during the Pleistocene.

The historical and pre-historical seismic records within the Alborz mountain range suggest the occurrence of strong earthquakes with often long-term recurrence intervals (e.g. Negahban, 1977; Ambraseys and Melville, 1982; Berberian, 1994; Talai, 1998; Berberian and

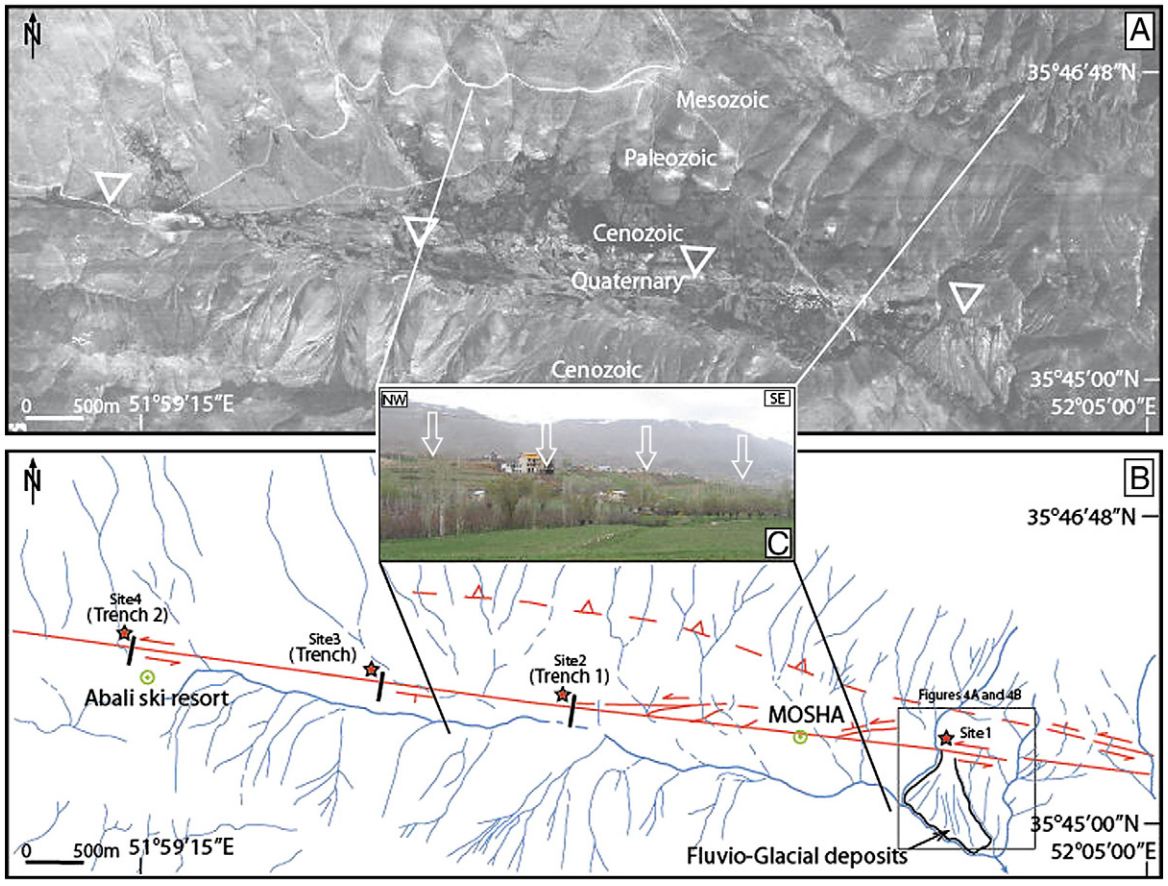

Fig. 3. Aerial picture (A) and its interpretation (B) of the East-Central Mosha fault within the Mosha Valley between Mosha and the Abali ski resort. Stars, blue lines, green circles and white triangles show respectively the sites, drainages, villages and active fault traces. North side of the site 1, the red dashed line remarks the western termination of the Eastern Mosha Fault. C: view towards the NE of The Mosha fault scarp within the Mosha valley. The scarp defines a straight alignment with 20–40 m difference in height.

Yeats, 1999, 2001). In the Tehran region, which was named initially Shahr-e Rey, several destructive historical earthquakes have been recorded since 958 AD. Earthquakes in 958 AD (Ms = 7.7, Io = X), 1177 AD (Ms = 7.2, Io = VIII+), 1665 AD (Ms = 6.5, Io = VIII+) and 1830 AD (Ms = 7.1, Io = VIII+) have been described in few studies such as Ambraseys and Melville (1982) and Berberian and Yeats (1999, 2001). The seismic events of 958 AD , 1665 AD and 1830 AD have been correlated to the Mosha, North Tehran and Taleghan faults at the north vicinity of Tehran region, respectively (e.g. Berberian and Yeats, 1999) (see Fig. 1). These destructive historical earthquakes show the important seismic hazard that the Iranian metropolis is facing nowadays. Two hundred years ago, in 1807 AD, the ancient Tehran was about 2 km^2 with 50,000 people. Today, Tehran and its suburbs areas represent a sprawling urban area of more than 1000 km^2, growing faster each day, where more than 15 million people are living.

3. Structural relationships and kinematics of the Mosha and North Tehran faults

The Mosha and North Tehran faults (see Figs. 1 and 2), are located at the southern border of the Central Alborz (see Figs. 1 and 2) and were first described by Dellenbach (1964) and Rieben (1955), respectively. Most of the pioneer works described the Mosha fault as a major reverse or thrust fault (e.g. Dellenbach, 1964; Allenbach, 1966; Steiger, 1966; Sieber, 1970; Tchalenko et al., 1974; Nabavi, 1976; Berberian, 1976; Berberian et al., 1985). Standing out in the highest part of the Central Alborz mountain range, the Mosha fault corresponds to the thrusting of the "High Alborz" (a complex folded zone of Paleozoic–Mesozoic and Tertiary formations) over the "Border Folds" to the south (Tchalenko et al., 1974). As for the Mosha fault, the North Tehran fault was first described as an active reverse fault controlling the thrusting of the Central Alborz reliefs above the Neogene foreland basin (e.g. Rieben, 1955; Dresch, 1961; Knill and Jones, 1968; Breddin, 1970; Tchalenko et al., 1974; Berberian et al., 1985).

Further studies allowed precising the recent kinematics of these two faults. Along the Mosha fault, mainly within its eastern part, several morphotectonic studies showed evidences of Quaternary left-lateral strike–slip faulting (Trifonov et al., 1996; Berberian and Yeats, 1999; Ritz et al., 2003; Solaymani et al., 2003; Allen et al., 2003b; Bachmanov et al., 2004; Ritz et al., 2006). These results are consistent with microseismic data showing active left-lateral movement along the eastern Mosha fault (e.g. Hedayati et al., 1976; Ashtari et al., 2005). Along the eastern Mosha fault, this left-lateral motion is associated with a normal component (Ritz et al., 2006) as also observed along the Taleghan fault (Nazari et al., 2009). This component is explained by the obliquity of the fault with respect to the general trend of the range (Ritz, 2009). There is no documented microseismic activity along the

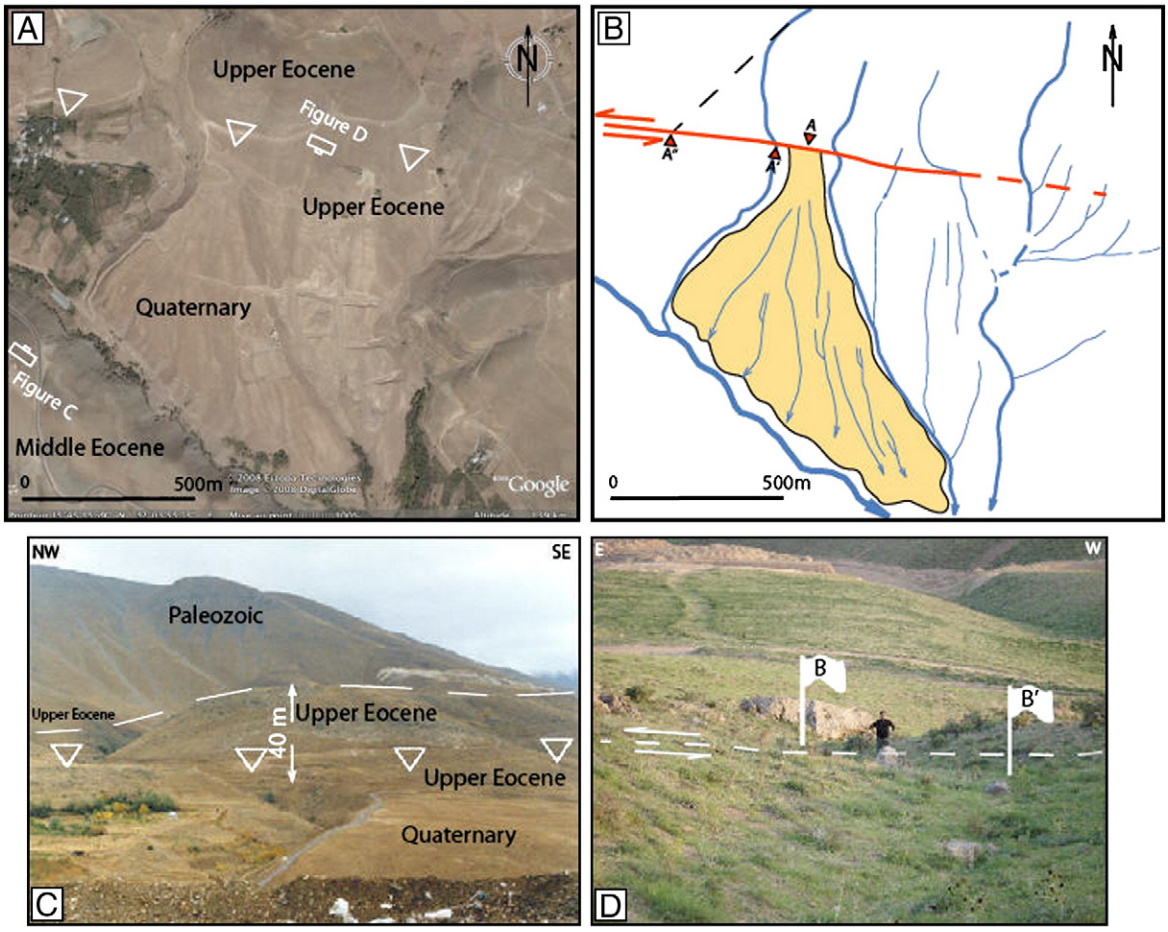

Fig. 4. Google earth image (from Cnes/Spot satellite with 2.5 pixel size) (A) and its interpretation (B) of the East-Central part of the Mosha fault (red line) at the eastern end of the Mosha Valley (site 1 in Fig. 3) showing the left-lateral displacement of an outwash cone. The blue lines reveal drainages. A corresponds to the apex of the cone. We define A′ and A″ as two piercing points reveal respectively the present-day and the most possible maximum value for location of the up streambed. A–A′ and A–A″ define the minimum and maximum offsets, respectively. The black dashed line shows the southward extension of the up streambed of the offset drainage. C: North–eastwards view of the Mosha fault scarp at the eastern part of the Mosha Valley (see figure A for situation). The triangles point out the trace of the Central Mosha fault. The white dashed line shows schematically the western termination of the Eastern Mosha fault trace (see the red dashed line north side of site 1 in Fig. 3). D: South–westwards view of a 5 m left-lateral offset drainage (B–B′) along the Mosha fault (see figure A for situation). We define B and B′ as two piercing points show the left-lateral offset.

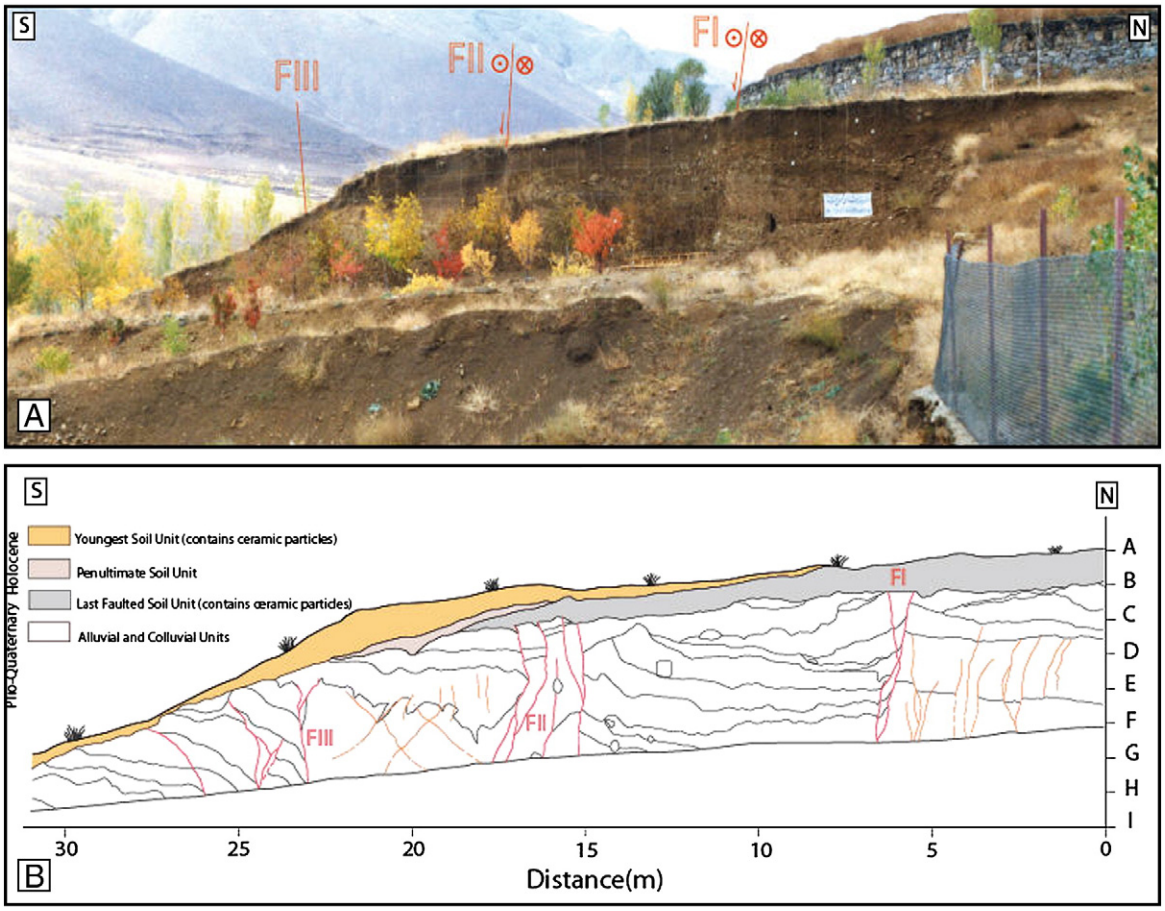

Fig. 5. Picture (A) and interpretation (B) of the east-facing artificial riser studied at site 2. The red lines correspond to ruptures along which are observed displacements. The orange lines define fractures without obvious displacements.

western section of the fault. Based on fault kinematics evidences found along this part of the fault, authors (e.g. Moinabadi and Yassaghi, 2007) described it as a thrust fault.

Along the North Tehran fault, Post-Pleistocene left-lateral component of motion was also suggested from the interpretation of the geometry of the faults within its NE–SW trending part, where three en-echelon branches are observed (Tchalenko et al., 1974). Further studies (Trifonov et al., 1996; Hessami et al., 2003; Bachmanov et al., 2004; Landgraf et al., 2009) presented some fault kinematics evidences of left-lateral deformation associated with the main thrusting movement along the North Tehran fault deduced from morphotectonic investigations. Along its western NW–SE section, the North Tehran fault shows clear morphological evidences of active thrusting (e.g. Berberian et al., 1985; Nazari, 2006).

In their recent work, using fault kinematics analysis, Landgraf et al. (2009) interpret the succession of three faulting regimes within the North Tehran and Mosha faults systems: a former dextral transpressional stage under a NW-shortening (just before Pliocene) was followed by a Pliocene to recent NE-shortening during which the North Tehran and Mosha faults formed a transpressional duplex. Finally, a sinistral transtensional youngest stage would have inverted the kinematics of the structures. The transition from first to the

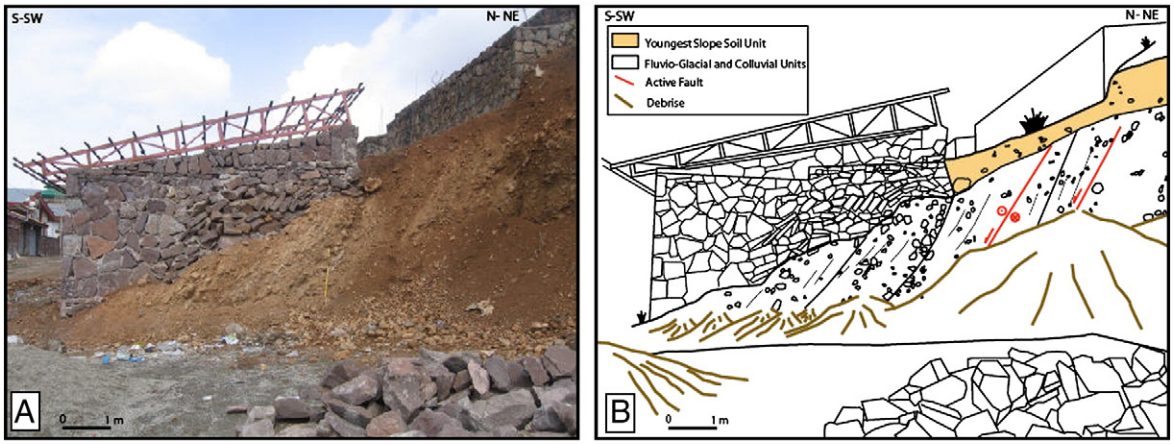

Fig. 6. Picture (A) and interpretation (B) of a section at the base of the Mosha fault scarp (site 3 in Fig. 3) showing Pliocene–Quaternary deposits affected by fault planes.

second stages is interpreted to be associated with the clockwise rotation of Shmax from NW–SE to NE–SW as it was previously proposed by Abbassi et al. (2003).

According to Abbassi and Farbod (2009) there is no geomorphological evidence for active faulting along the North Tehran fault as defined classically at the mountain front zone of Tehran. The active deformation seems, instead, to have switched southwards within the Niavaran, Lavizan and Tarasht faults (see Fig. 1). The Niavaran fault was first recognized by Dellenbach (1964) and by Tchalenko (1975), which is situated ~1 km southwards the NTF and is roughly parallel to it. Berberian et al. (1985) and Berberian and Yeats (1999) mapped the fault as a 12 km long, north-dipping steep thrust fault. In his 1985 report, Berberian presented some evidences of left-lateral horizontal component along the eastern part of the fault. In its western part, Abbassi and Farbod (2009) described active left-lateral strike–slip features associated minor normal faults situated northwards of the Niavaran fault. According to Abbassi and Farbod (2009), the thrusting deformation is now occurring south of the Niavaran fault, along the roughly E–W trending Lavizan and Tarasht faults.

4. Morphotectonic analysis along the Central Mosha and North Tehran faults

We studied the central part of the Mosha fault and its junction zone with the eastern section of the North Tehran fault within nine different sites (Fig. 2). The central part of the Mosha fault can be defined as the portion of the fault extending from Mosha village to Shahrestanak village (Solaymani et al., 2003). Along its central part, the fault shows a smooth deviation in strike at Lavasanat area. West of this area, the strike of the Mosha fault is 130°E whereas east of it, the fault is striking 110°E. In this paper, we name these two parts West-Central and East-Central Mosha faults, respectively. The junction of the NTF with the Central Mosha fault sets at the bend between the West- and East-Central Mosha faults. Our study was first based on the interpretation of aerial photographs. We used the oldest set of photographs (1955) to work on Quaternary landscapes preserved from the effects of the recent increase of human activities in the region. Our preliminary morphotectonic mapping was then completed by field studies. The detailed mapping combined with morphological field observations permit details of fault trace, geometry and kinematics to be deciphered. These observations have also allowed us to study the relationship between geomorphological features and fault kinematics.

4.1. The Central Mosha fault within the Mosha valley

The Mosha valley is situated at the eastern part of the East-Central Mosha fault and corresponds to a glacial valley with fluvio-glacial and colluvium deposits that can be attributed to the Würm and Riss periods from stratigraphical observations of the western end of the valley (Pedrami, 1983). These Quaternary sediments are affected by a linear fault scarp defining a steep dipping fault between the Mosha village and the Abali ski resort (Fig. 3A and B). The scarp defines a straight alignment with a difference in height of 20–40 m between the northern and the southern parts (Fig. 3C). This main Quaternary rupture re-activates an older structure separating Paleozoic and older formations to the north from Eocene (Karadj formation) and younger formations to the south. Within the eastern part of the valley, several small N070°–080°E trending sinistral fault branches connect the main N100°E trending linear scarp (Fig. 3B). From fault slip data strike, dip/dip-direction and dip-slip component/rake, are 075, 80S, −2, respectively. The fact that the height of the main fault scarp is a little (~10 m) higher to the east than to the west can be related to these secondary

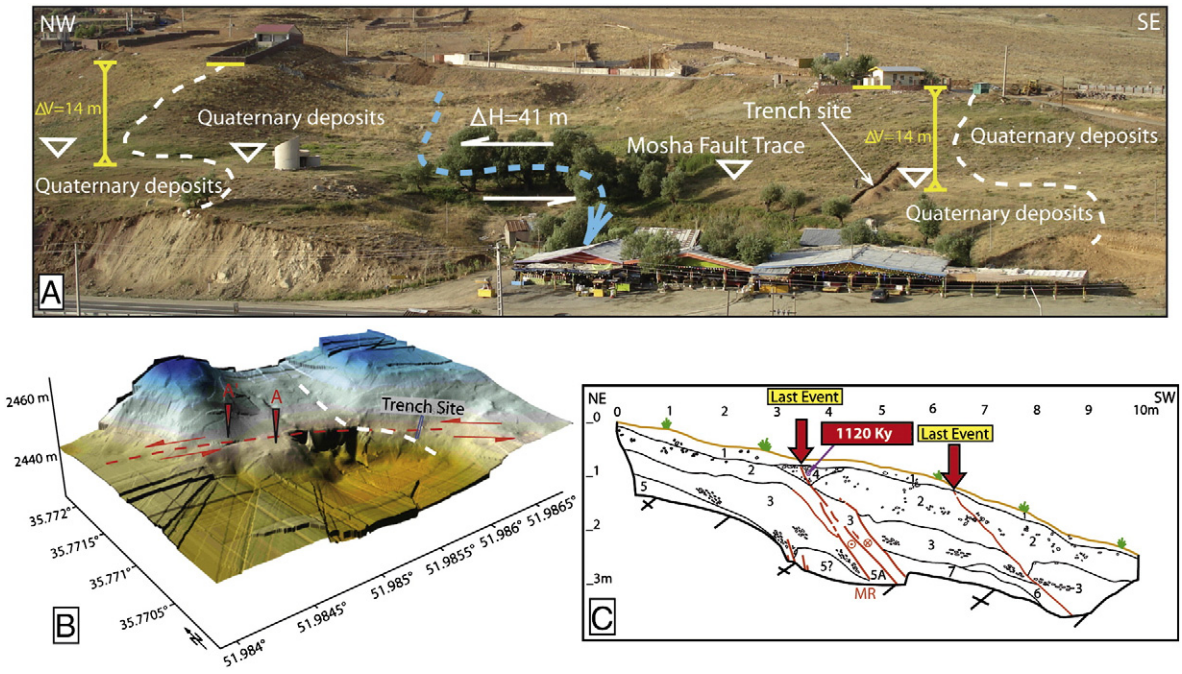

Fig. 7. Photo (A) and DEM calculated from D-GPS (Differential Global Positioning System) surveying (B) of the two ridges left-laterally displaced in Quaternary deposits, west of Abali ski resort (Mosha fault; Site 4 in Fig. 3). In figure A: the white and blue dashed lines show schematically the axial position of two deformed ridges and their related drainage, set perpendicular to the fault trace (white triangles), respectively. In figure B: the left bank of the offset drainage (marked by white dashed line) helps us to identify more clearly the eastern Shutter ridge. We define A and A′ as two piercing points to estimate horizontal offset. To estimate the values of horizontal and vertical displacements we profited from Topography and fault slip data calculation. C: log of the trench opened across the Mosha fault scarp westwards of Abali ski resort. The red lines correspond to ruptures with displacements. MR: main rupture. Here, based on Optical Stimulation Luminescence (OSL) dating of the unit 4 as the last event-horizon unit, we identified the maximum age of the last seismic event (see text for more information). Description of the units found on trench wall: unit 1; superficial soil-rich of organic materials contains some pebbles, unit 2; sub-superficial soil-poor of carbonate and contains pebbles, unit 3; slope unit contains bad sorted angular coarse pebbles, unit 4; sandy–silty unit contains some angular particles in centimeteric size, generally defined as a faulted colluvial wedge, unit 5; yellowish silty unit, unit 5A; unit 5 within the main fault zone, unit 6; slope unit contains bad sorted angular coarse grains, and unit 7; beige fine grain unit contains some pebbles.

features. This eastern section of the fault scarp is also characterized by the occurrence of surficial travertines indicating water circulation within the fault zone.

The intensive agricultural activities during the last decades and the recent building constructions have modified and erased most of the recent morphological features, precluding the possibility of evidencing easily kinematics indicators at large scale. However, clear features of left-lateral strike–slip faulting can be observed east of the Mosha valley within the overlapping zone between the central and eastern portions of the fault (site 1, Fig. 3A and B). There, a cone made of glacial out-washes shows a cumulative left-lateral displacement comprised between 140 (A–A′ in Fig. 4A and B) and 390 m (A–A″ in Fig. 4A and B) (mean value: 265 ± 125 m).

Fig. 4C shows a north–eastwards view of the Quaternary outwash deposits. The difference in height between the erosional surface within the bedrock to the north and the surface of the outwash deposits to the south is ~40 m. We assume that this value corresponds to the vertical offset of the fault postdating the deposition of the debris cone. Offset of streams incisions show left-lateral displacements of 5 m, 30 m and 75 m (Fig. 4B and D).

Three kilometers westwards, within a small hill located on the upper part of the fault scarp, we cleaned an east-facing artificial riser made for agricultural purpose (site 2 in Fig. 3). For logistical and administrative reasons, we could not open a long trench reaching the toe of the fault scarp. The study of this 32 m long west wall shows a 25 m wide faulted zone capped by a flat abrasive unit mainly composed of sand and silt from which developed a soil unit (Fig. 5A and B). Two main faulted zones with south dip-direction can be observed: to the north, one observes a steep south-dipping rupture (FI). This rupture is sealed by the organic-rich sandy–silty unit in which we found ceramic fragments. Slickensides along the rupture plane characterize a sinistral movement with a small normal component (075, 80S, -28), which is also observed immediately to the north along parallel secondary planes (070, 74S, -28). To the south, we observed two sets of ruptures. A first set of ruptures (FII), dipping steeply to the south, cuts the Holocene soil unit containing ceramic fragments and show fault slip data (103, 81S, -09) indicating left-lateral strike–slip fault with a small normal component. A second set (FIII) is dipping steeply to the north. In terms of strike, the steep fault planes (FII) correspond to the main scarp direction observed in the morphology (N100°E), while the fault planes observed within FI seem to correspond

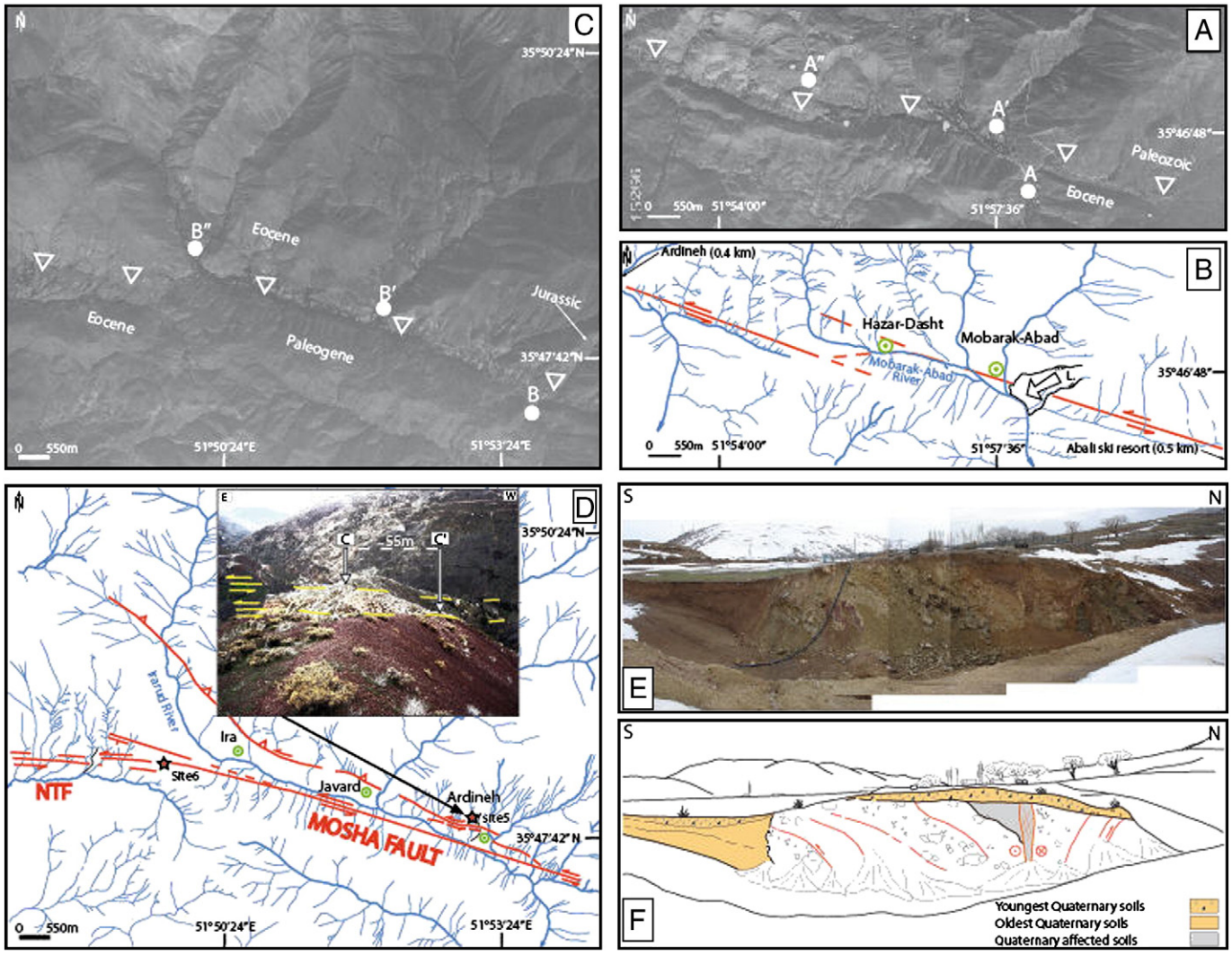

Fig. 8. Aerial photograph (A) and its interpretation (B) of the Mosha fault within the Mobarak-Abad region, between Abali ski resort and Ardineh. A–A′ and A–A″ define the minimum and maximum offsets, respectively. The fault trace marked by white triangles. L: Mobark-Abad landslide. C and D show respectively aerial photograph and its interpretation of the Mosha fault zone within the Ardineh-Ira valley, between Ardineh and Ira villages. Here, B–B′ and B–B″ define the minimum and maximum offsets, respectively. In figure D, the picture shows south view of the double-shutter-ridge within the Pliocene–Quaternary deposits, north of Ardineh village (C–C′ ~55 m). The yellow dashed lines remark the fault traces. Field picture (E) and interpretation (F) of a positive flower structure observed west of Ira village.

to the N75°E trending riddle planes oblique to the main line FII. This pattern is consistent with our plan-view interpretation of the fault traces (see Fig. 3B).

Westwards, 1.5 km from site 2, at the base of the fault scarp where new buildings were under construction, we found a section across Pliocene–Quaternary deposits (site 3 in Fig. 3B). Within this NNE–SSW section, we observed two faults dipping 52°S and cutting through detrital material dipping ~60–65°S (Fig. 6A and B). Striation measurements along the two faults (096, 52S, -44) attest for a left-lateral-normal motion.

Westwards of site 3, immediately to the west of the Abali ski resort, the stereo analysis of the 1/20.000 and 1/10.000 scale aerial photographs allowed finding another evidences for two left-laterally offset ridges along the Mosha fault (site 4 in Fig. 3B). These features are not obvious to observe today because of human activity (road, agriculture, and buildings) that modified the original morphology (Fig. 7A). Fig. 7B shows the DEM obtained by surveying the site with GPS kinematics. From the DEM, we determined a left-lateral horizontal offset of a 41 ± 4 m and a vertical offset of 14 ± 1 m as shown by the shifting of the ridges and the stream risers, yielding a ratio H/V of ~3 (Fig. 7B). We measured a strike of N100°E and a dip of 70°S for the main rupture in a trench excavated across the fault scarp (Fig. 7C, see location in Fig. 7A and B). Combining H, V and the dip allowed us to calculate a rake of −20°. The dating of the colluvial unit 4, the most recent unit affected by the fault, allows us to estimate the elapsed time since the last rupture along the fault. OSL dating that relies the time elapsed since the last sunlight exposure of a Quartz-rich sandy layer yielded an age of ~1120 years for unit 4. The last earthquake could correspond to one of the two historical seismic events that occurred in 1665 AD and 1830 AD, with a preferred interpretation for the 1830 AD earthquake taken the meizoseismal areas (e.g. Berberian and Yeats, 1999; see Fig. 1).

4.2. The Central Mosha fault between Abali ski resort and Ardineh

Between Abali ski resort and Ardineh village, the active parts of the Mosha fault zone define two 110°E trending left-lateral left-stepped en-echelon fault branches (Fig. 8A and B). These branches cut through or reactivate ancient thrusts faults between Paleozoic and younger formations. East of Mobarak-Abad village, the fault trace is covered by an active landslide that could have been triggered during the October 2, 1930 (M = 5.2) earthquake, event during which several landslides occurred in the nearby Ardineh-Ira valley (see Ambraseys and Melville, 1982; in this reference the Ardineh valley is named the Ira-rud valley).

West of Hazar-Dasht, several small left-lateral offset features are observed, and the shape of the Mobarak-Abad River suggests a left-lateral cumulative displacement comprised between 0.8 (A–A′) and 3.8 km (A–A″) (Fig. 8A).

4.3. The Central Mosha fault between Ardineh and Ira

Between Ardineh and Ira, Ira-Rud River runs linearly and seems to be controlled by the N110°E trending strike of the Mosha fault which generally separates the Jurassic and Eocene (in the north) from the Paleogene formations to the south (Fig. 8C and D). Large scale offset features within the drainage indicate a cumulative left-lateral displacements of ~3 km (B–B′). The total cumulative left-lateral slip cannot correspond to the ~6 km between points B and B″, because the catchment basin upstream B″ is too small. North of this main left-lateral strike–slip linear segment, we observe a parallel branch along which the deformation is also left-lateral and would evolves gradually to oblique left-lateral-reverse considering the gradual change of strike from N110°E to N130°E.

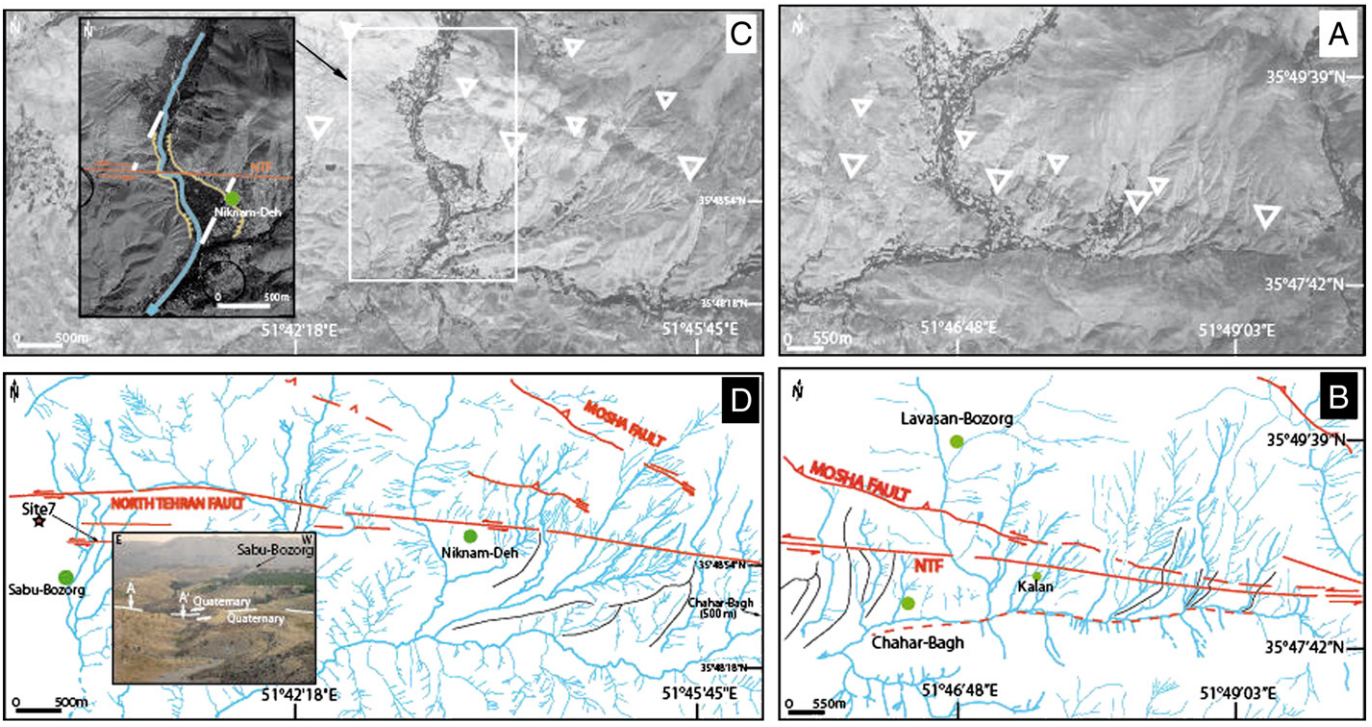

Fig. 9. Aerial photo (A) and its interpretation (B) of the overlapping zone between the Central Mosha and North Tehran faults (NTF) within the eastern Lavasanat area. The fault traces marked by white triangles (on aerial photos) and red lines (on interpretations). In figure B, the red dashed line shows a postulated fault trace. Aerial photo (C) and its interpretation (D) of active features observed along the North Tehran fault between Chahar-Bagh and Sabu-Bozorg in the Lavasanat area. In figure C, the picture shows enlarged aerial photograph of the North Tehran fault trace westwards from Niknam-Deh village with main morphotectonic features: the white dashed lines define the maximum left-lateral offset (900 m) estimated from the deflection of the river. Site 7: within the figure D, the picture shows southwards view of a left-laterally offset drainage and interfluve at the north-eastern vicinity of Sabu-Bozorg village within the central Lavasanat area (A–A′ ~40 m). Within the picture, the white dashed line shows the traces of North Tehran fault.

Field observations in the eastern part of the Ardineh-Ira valley allowed us to better constrain the kinematics of recent faulting in this area. Site 5 is located where we interpreted the occurrence of two parallel active branches from detailed observations (see Fig. 8C and D). This site is located on the northern branch, just to the north of Ardineh village within the Pliocene–Quaternary deposits. There, we observed a topographic ridge shuttered left-laterally by two parallel rupture lines (photo presented in Fig. 8D) cumulating together a horizontal displacement of ~55 m (C–C′). We estimated also a vertical offset of ~18 m, which yields a ratio H/V of ~3.

4.4. The junction zone between the Central Mosha and eastern North Tehran faults

From 51°50′24″E westwards, the left-lateral strike–slip deformations observed along the Central Mosha fault stepped to the left within left-stepping branches bending progressively to the west (see Fig. 8D). We consider that this left-stepping pattern corresponds to the junction zone between the active Mosha fault and the active North Tehran fault (NTF). One kilometer west of Ira, we observed a symmetric hump in the morphology cut by a trench (site 6, see Fig. 8D). This artificial section shows a fault zone displaying several ruptures between bedrock (Eocene formations) and Quaternary reddish soil units (Fig. 8E and F). Fault slip data (105, 83 N, 33) within the vertical ruptures indicate sinistral slips associated with a reverse component. Considering this kinematics data together with the general rupture pattern, we interpret the overall feature as positive flower structure associated with a main left-lateral strike–slip deformation.

Further west, towards Chahar-Bagh sets the eastern Lavasanat area. Our aerial photographs interpretation allows characterizing an overlapping zone of ~3 km length between the Central Mosha fault and the eastern termination of the NTF (Fig. 9A and B). Westwards Kalan village, we observed several left-lateral offset features within drainages and ridges along a ~N105°E trending linear trace corresponding to the NTF (see Fig. 9A and B). In this area (located within the western part of the Fig. 9A and B),cumulative horizontal slip of the drainage just north of Chahar-Bagh, the two western drainages limited the deformed ridge and the main river risers varies from 80, 330 to ~600 m, respectively.

To the north of the North Tehran fault, it is difficult to conclude about activity along the West-Central Mosha fault and its kinematics. Within this area, because of steep reliefs, evidences of Quaternary features are limited compared to the area around the East-Central Mosha fault. Few morphotectonic features (deformed drainages and ridges) suggest that the active left-lateral deformation continues

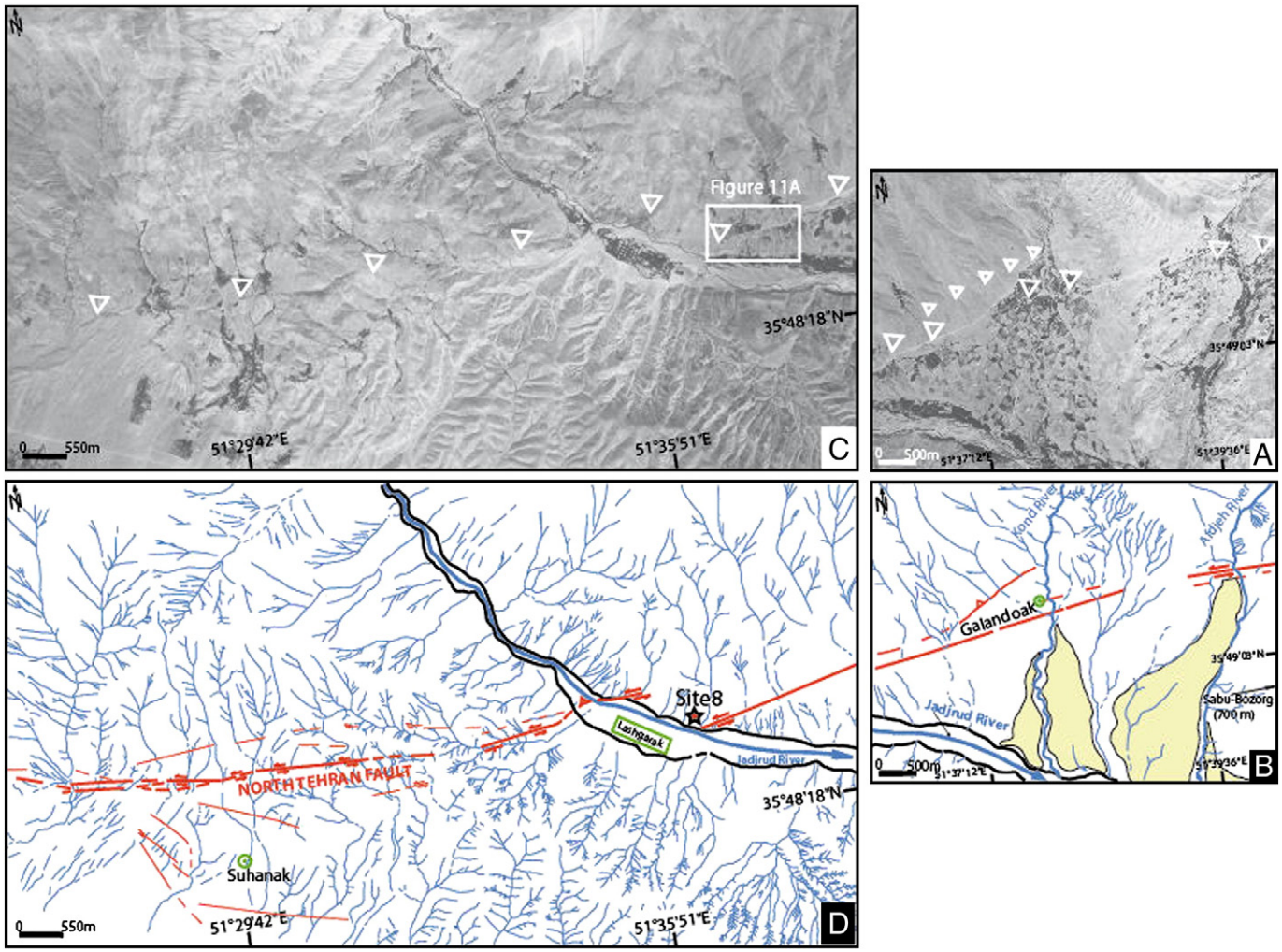

Fig. 10. Aerial photograph (A) and its interpretation (B) of the North Tehran fault zone within the western part of the Lavasanat area. The yellowish surfaces show the Pliocene–Quaternary alluvial fan deposits associated with the Afdjeh and Kond rivers. Aerial photograph (C) and its interpretation (D) of the North Tehran fault zone within the Lashgarak-Suhanak region. The thick black lines show the risers of Jadjrud River. In the overlapping zone of the fault branches, this main river has a wide bed that is probably a result of concentrating erosion within the fault zone as a weak domain.

westwards along a rupture bending from ~N105°E to N130°E. Considering this bending, the kinematics of this section of the Central Mosha fault (West-Central Mosha fault) would evolve gradually from mainly left-lateral to oblique reverse-left-lateral. Further north–westwards, we observed clear morphological and kinematics evidences of oblique reverse-left-lateral deformations within the Quaternary deposits. Slickensides along the rupture plane (at 35° 51′ 38.15″N, 51° 40′ 24.39″E) characterize a thrust movement with a sinistral component (305, 70N, 65).

4.5. The eastern NTF within Lavasanat area between Chahar-Bagh and Galandoak

Within the central Lavasanat area, between Chahar-Bagh and Sabu-Bozorg villages the alignment of several offset streams and ridges define the active trace of the eastern NTF (Fig. 9C and D). This active trace corresponds generally to the tectonic contact between Eocene and Pliocene–Quaternary formations. The trace of the fault can be followed from Chahar-Bagh to Niknam-Deh villages and further west. Its linearity indicates that the fault plane has a steep dip. West of Niknam-Deh village, the large scale deflection of a river indicates a cumulative left-lateral displacement of ~900 m (enlarged aerial photo in Fig. 9C), while the present river bed shows a deflection of ~200 m.

West of 51°42′18″E, the trace of the fault bends slightly from N095°E to N085°E, and several parallel ~1–2 km long fault strands can be traced southwards of the main trace. One of these parallel strands is located at the north-eastern vicinity of Sabu-Bozorg village (site 7 in Figs. 2 and 9D) and corresponds to the offset of two drainages and their interfluve. We estimated the horizontal and the vertical cumulative displacements to be ~40 (A–A′) m and ~10 m, respectively (photo in Fig. 9D).

Due to the modifications of the landscape by human activities within the western Lavasanat area, the trace of the NTF is difficult to follow on the morphology. Fig. 10A and B show an interpretation of the morphology within the Galandoak city. In the eastern part of the 1955 aerial photograph, the Afdjeh river shows a deflection feature indicating a cumulative left-lateral displacement of ~1200 m matching the westwards extension of the NTF mapped in Sabu-Bozorg village (see Fig. 10B).

4.6. The NTF within the northeast of Tehran City

West of the Jadjrud River, between Lashgarak and Suhanak, several evidences for left-lateral strike–slip faulting can be observed in the morphology (Fig. 10C and D). Within the Jadjrud River, the trace of the fault is rather simple with two branches trending N075°E and defining a right-stepping system. Within the overlapping zone of the fault branches, Jadjrud River has a wide streambed that is probably the result of a stronger erosion within the fault zone. Further west, towards Suhanak, the active traces are more complex and define a fault zone displaying several straight branches.

Kinematics indicators are observed within the Jadjrud River. Along the eastern branch (site 8 in Fig. 10D), active faulting is localized within a narrow fault zone, showing left-laterally offset drainages

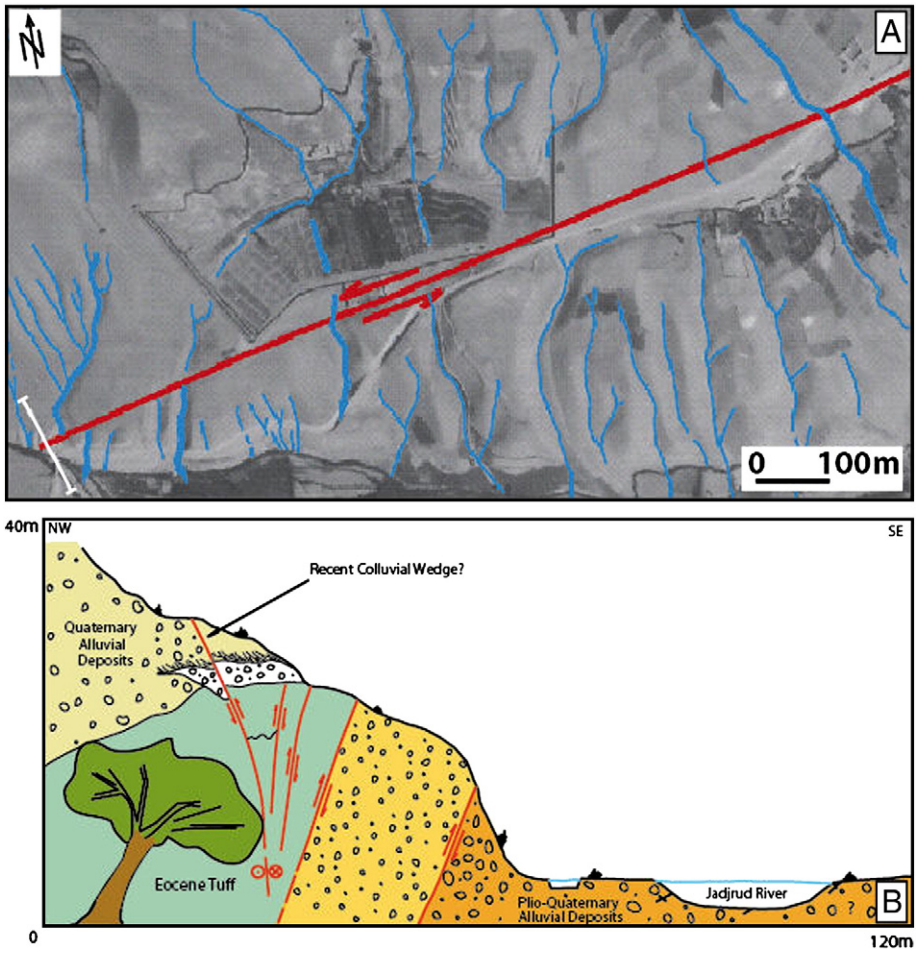

Fig. 11. (A) Enlarged aerial photo with interpretation of morphotectonic features along the North Tehran fault, east of Lashgarak (see Fig. 10C for situation). The white solid line indicates the cross section presented in figure B. Here, active faulting is localized within a narrow fault zone, showing left-laterally offset drainages. Figure B shows a schematic cross section of the North Tehran fault scarp within Jadjrud River (site 8 in Fig. 2); see text for details.

(Fig. 11A). Fig. 11B represents a cross section at the western tip of the fault branch showing a set of steep north-dipping contacts affecting the Eocene Karadj formation and Pliocene–Quaternary deposits. Taken the left-lateral movement observed in the morphology (Fig. 11A) and the structures pattern observed in cross section (Fig. 11B), we interpret the overall features as a positive flower structure associated with the active left-lateral strike–slip deformation along the fault.

The western branch shows a northern dip when it crosses the Jadjrud River but a southern dip further west. Evidences of left-lateral strike–slip movements have been preserved within the left bank of Jadjrud River showing a horizontal displacement of about 100 m (Fig. 10D), and further west where small drainage shows also horizontal deflections indicates a cumulative left-lateral displacement of ~25 m.

4.7. The NTF within the northeast of Tehran between Suhanak and Darabad

Between Suhanak and Darabad villages, within the northeastern Tehran region, at the western end of the Lashgarak linear valley, the active tectonics features corresponding to the NTF are distributed on several strands defining a general ~E–W trend (Fig. 12A and B). Left-lateral offset features are observed in the morphology ~1 km northwards of Suhanak village, where several streams and ridges are left-laterally shifted with a displacement of about ~150–200 m (Fig. 13A and B). No obvious vertical component seems to be associated with this left-lateral strike–slip deformation.

At Darabad village, the active left-lateral movement observed along the NTF is transferred along the Niavaran fault, looking as a right-stepping en-echelon of the NTF. Based on aerial photos investigation, evidences for recent deformation keep straight across Tehran City along the Niavaran fault, with morphotectonic features (e.g. offset terrace risers) indicating left-lateral strike–slip displacements larger than 500 m (Fig. 13C).

No clear evidence of present-day activity is noticed along the NTF (except near Karadj; see Section 3) strictly speaking, classically mapped as a thrust fault following the sinuosity of the southern mountain front. Fig. 14A and B show the north-dipping NTF, 1 km west of Jamaran (site 9, Fig. 12), cutting through the andesitic tuffs layers of the Karadj formation, Eocene in age, and Quaternary colluviums. Fault slip data (277, ~70N, 23) within the steeped Quaternary rupture indicate a sinistral slip associated with reverse component. This evidence of active faulting found at a portion of the North Tehran fault that is situated semi-parallel to the trace of active Niavaran fault. Nearby this site, a rock avalanche seems to be affected by the fault scarp (see Fig. 12A and B) but this feature observed on aerial photograph could not be confirmed in the field, because of building constructions.

Except these few evidences of quaternary faulting, our investigations along the NTF zone revealed that, generally the tectonic activity does not follow the older trace of the fault corresponding to previous long-term dip–slip thrusting movements. The recent faulting mainly occurs on new traces trending E–W to ENE–WSW and affects Quaternary features (streams, ridges, risers, and young glacial markers) cutting straight through the topography.

5. Discussion and conclusions

In this paper, we clarified both the present-day structural relationships and kinematics of the Mosha and North Tehran faults at their junction. The Mosha and North Tehran active traces affect Quaternary features such as Late Pleistocene glacial markers, streams, ridges and terrace risers. Cutting straight across the topography, these traces define

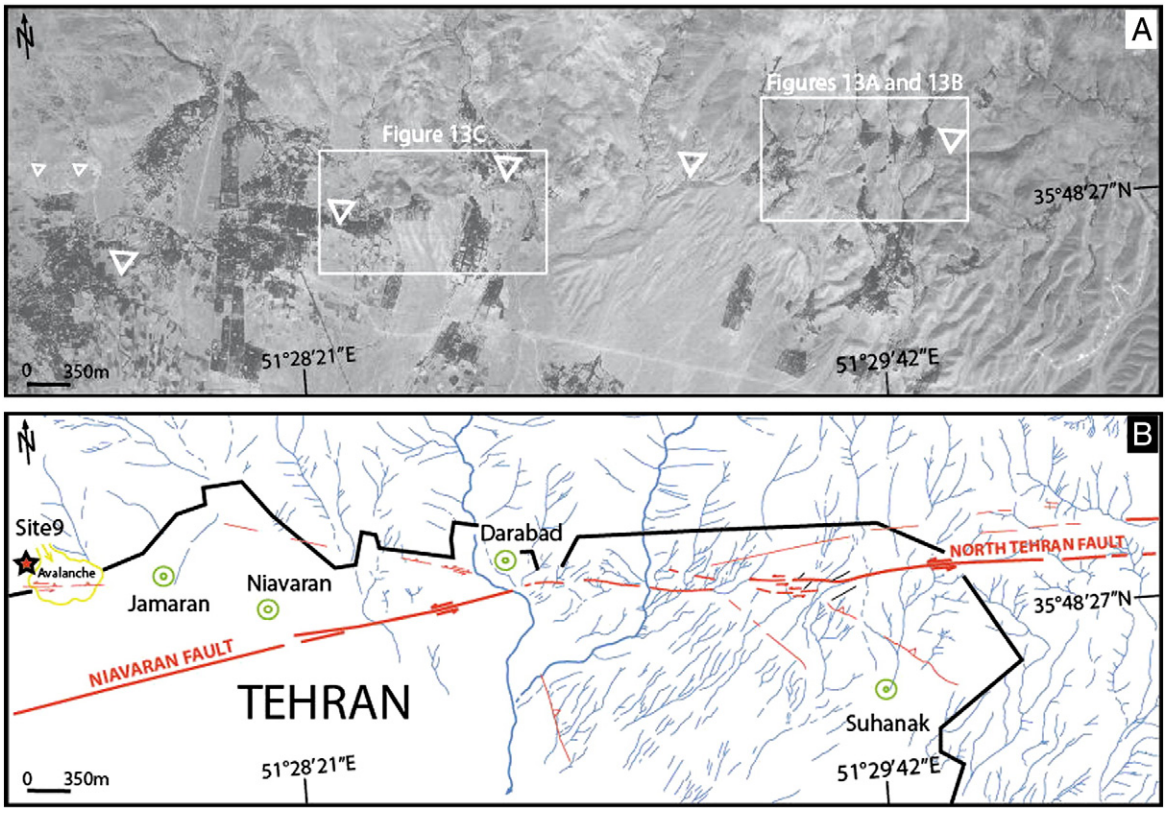

Fig. 12. Aerial photograph (A) and its interpretation (B) of the North Tehran and Niavaran faults northeast of Tehran. At Darabad village, the active left-lateral movement observed along the North Tehran fault is transferred along the Niavaran fault, which appears as a right-stepping en-echelon of the North Tehran fault. The site 9 is located along the North Tehran fault zone at the mountain front domain, which affects potentially a rock avalanche (the yellow line). The thick black line marked the boundary of Tehran City in study area.

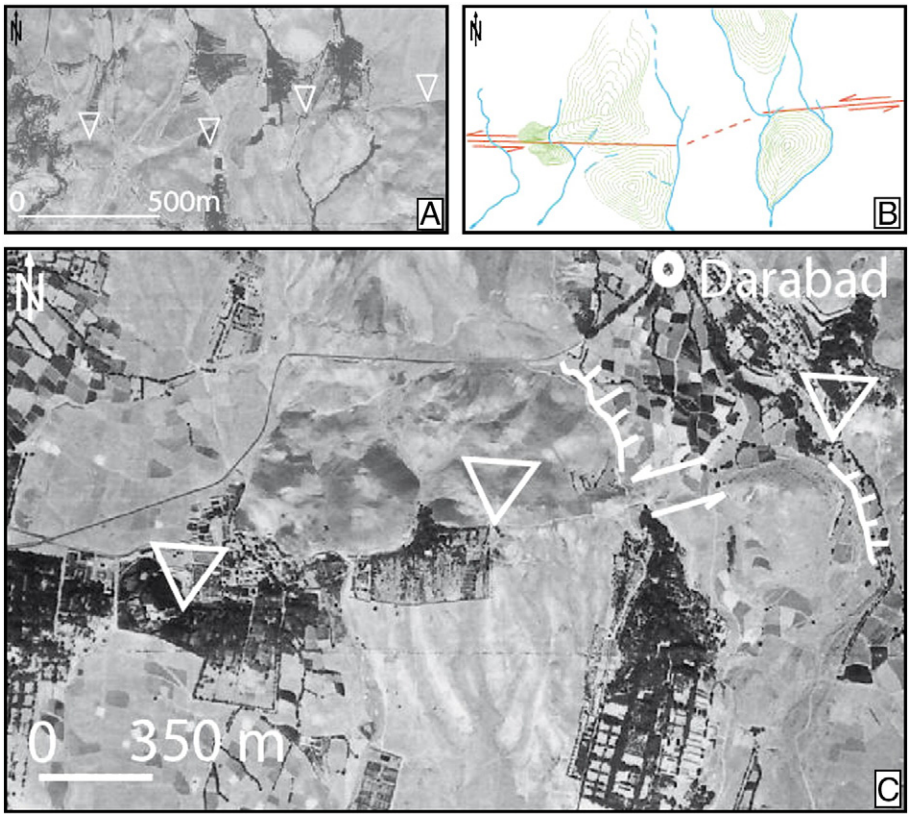

Fig. 13. Enlargement of the North Tehran fault trace (white triangles) on aerial photo (A) and its interpretation (B) shows en-echelon geometry north of Suhanak village. Here, the drainage beds (blue lines) and ridges (green centroid lines) offset clearly left-laterally (~150–200 m). Figure C shows aerial photograph of the Niavaran fault. Note the left-lateral offset (>500 m) of the terrace riser (patched white line) along the fault trace marked by white triangles.

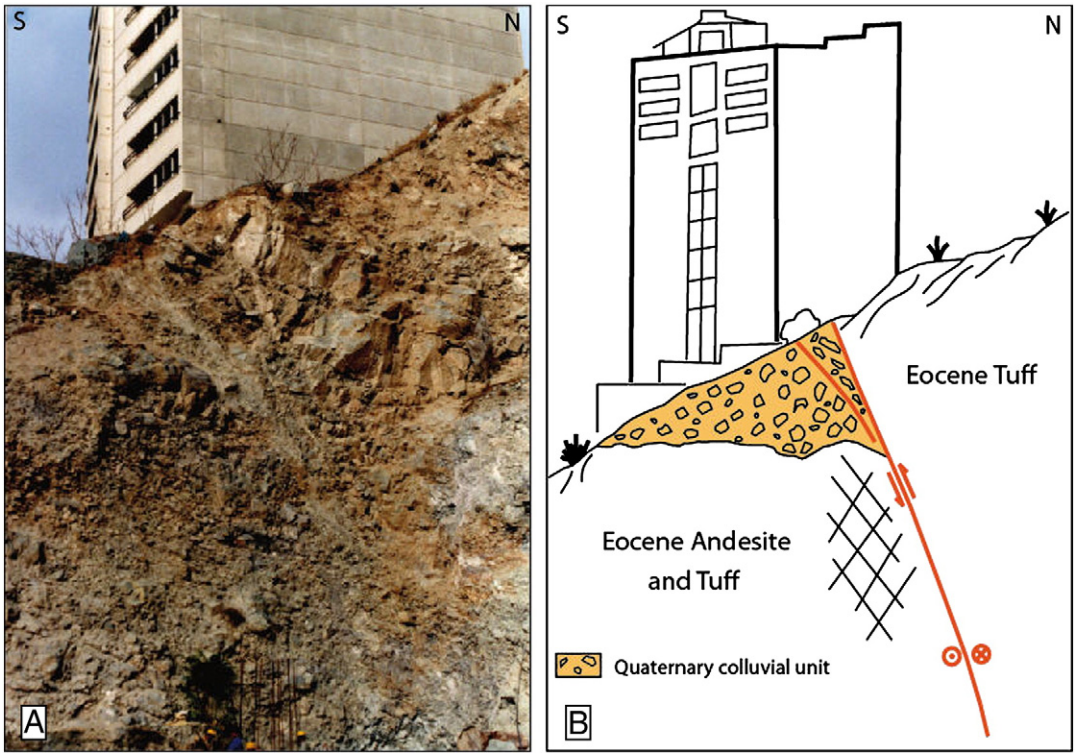

Fig. 14. Picture of a quarry (A) and its interpretation (B) showing the North Tehran fault 1 km west of Jamaran (site 9 in Figs. 2 and 12B). Note the steep north-dipping shear zone in the Eocene tuffs (Karadj formation) affected the Quaternary surficial unit, with brecciation of the layers near the fault plane.

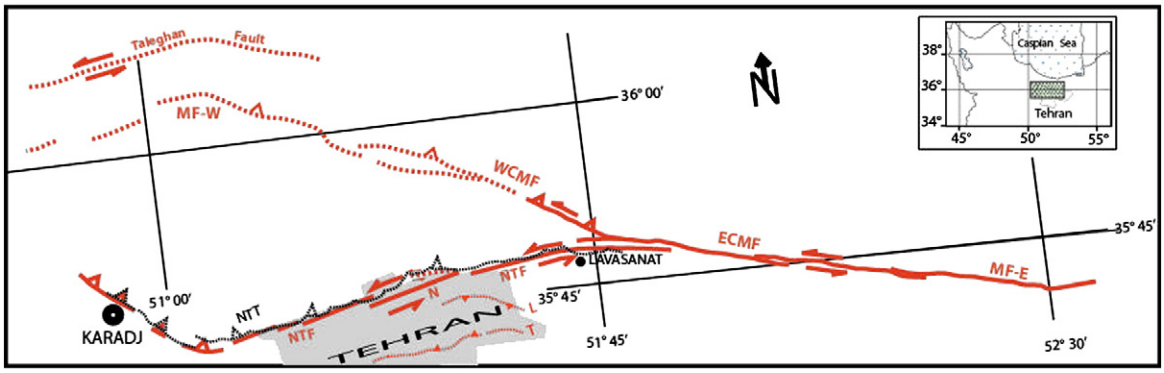

Fig. 15. Sketch map of active faulting within the northern Tehran region. The traces of activity within our study area (red solid lines) generally do not follow the older traces corresponding to previous long-term dip–slip thrusting movements (black dotted line with NTT for the North Tehran Thrust). The recent faulting movements occur on new traces trending from WNW–ESE to the east to WSW–ENE to the west, affecting Quaternary features. NTF: North Tehran Fault, N: Niavaran fault, L: Lavizan fault and T: Tarasht fault (L and T locations after Abbassi and Farbod, 2009). The red dotted lines show the faults that located out of our study area.

steep faults with either north- or south-dipping directions, along which clear evidences of left-lateral strike–slip faulting are found.

Evidences of predominant active left-lateral strike–slip faulting are found from the eastern Mosha valley to the Tehran City, all along the junction zone between the Mosha and the North Tehran faults. Eastwards of the junction zone, within the Mosha valley (site 1) and around Ardineh village (site 5), we estimated a ratio between horizontal and vertical displacements (H/V) of ≥ 3. This result differs from previous studies that estimated ratios of ~2 and ~1 for H/V at these same sites, respectively (Trifonov et al, 1996; Bachmanov et al., 2004). The difference of interpretation is even larger when one considers that the vertical displacement corresponds generally to a normal component and not a reverse component as interpreted by the previously mentioned authors. This local slight transtensional deformation is generally associated to left-stepping en-echelon pattern. It is explained by the obliquity of the WNW–ESE trending Central Mosha fault zone with respect to the general NE–SW trend of the range (Ritz et al., 2006; Ritz, 2009; Nazari et al., 2009).

The left-lateral strike–slip motion is then transferred westwards along the eastern North Tehran fault zone bending progressively from WNW–ESE to WSW–ENE. There, newly-formed fault branches show right-stepping en-echelon pattern suggesting local transpressional deformation. One of the main right-stepping en-echelon features occurs between the eastern part of NTF and the Niavaran fault, a left-lateral strike–slip WSW–ENE trending fault, crossing straight across the northern part of the Tehran megacity. This right-stepping en-echelon left-lateral strike–slip fault pattern would extent further west until the Karadj region, where are observed active NW–SE trending thrust faults (Nazari, 2006).

Our investigations show that along the eastern part of the Central Mosha fault, the traces of recent activity follow generally older structures. On the other hand, recent faulting features do not often follow the previous long-term dip–slip thrusts along the North Tehran fault at the foothills of the reliefs but instead occur on new traces trending WSW–ENE (Fig. 15). This result differs from Landgraf et al. (2009) who interpreted a sinistral component along the geological trace of the eastern NTF.

The cumulative offsets associated with this left-lateral deformation is small compared with the topography associated with the previous Late Tertiary thrusting motion, suggesting a recent change of fault kinematics. This is consistent with the interpretations of several works that described similar changes of kinematics from mainly reverse to mainly left-lateral at local scale (e.g. Abbassi and Shabanian, 1999; Solaymani et al., 2003; Abbassi and Farbod, 2009). This change correlates well also with the regional model proposed by Ritz et al. (2006) and Ritz (2009) for the South Caspian region and Alborz. In our study, we estimated ~3 km of cumulative left-lateral displacement along the Central Mosha fault between Abali and Ira (see Fig. 8A and C). This is the same cumulative offset than Ritz et al. (2006) estimated along the eastern Central Mosha fault, from which they inferred an age of 1–1.5 Ma for the kinematical change by dividing the 3 km of cumulative offset to 2.2 mm/year horizontal slip rate. The same timing is proposed by Nazari et al. (2009) along the Taleghan fault, by dividing the 450 m observed cumulative vertical deformation by a 0.5 mm/year vertical slip rate. The cumulative left-lateral offsets that we observed along the NTF is lower (0.6 to ~1 km) than along the Mosha fault (~3 km) suggesting either that the kinematic change has propagated from east to west, or that the left-lateral slip rate decreases from east toward west.

Our observations are also consistent with geodetic data (Djamour et al., 2008) showing that the southern Central Alborz is mainly characterized by left-lateral inter-seismic deformation rather than vertical deformation.

At last, our study highlights at different way the question of the source for the past 1830 AD, Ms 7.1 historical earthquake, interpreted classically as being associated with the Western Central Mosha fault (Berberian and Yeats, 1999). Our observations suggest that its mechanism was left-lateral and its source probably closer to Tehran than proposed earlier, within the junction zone between the Mosha fault and the North Tehran fault.

Acknowledgments

This work was supported by the International Institute of Earthquake Engineering and Seismology (IIEES) and the laboratory of Geosciences Montpellier of the University Montpellier 2. We are grateful to M. Osati and I. Zahedi for their logistics help in the field, and to F. and M. Kushki for digging the trench in Abali. We thank H. Tabassi, E. Shabanian, M. Foroutan and K. Fegghi for the fruitful discussions, and S. Mahan for the OSL dating of unit 4 in the Abali trench.

References

Abbassi, M.R., Farbod, Y., 2009. Faulting and folding in Quaternary deposits of Tehran's piedmont (Iran). Journal of Asian Earth Science 34, 522–531.

Abbassi, M.R., Shabanian, B.E., 1999. Evolution of the Stress Field in Tehran Region during the Quaternary: S.E.E. 3 Meeting, Tehran, vol. I, pp. 67–77.

Abbassi, M.R., Shabanian, B.E., Farbod, Y., Feghhi, Kh., Tabassi, H., 2003. The State of Contemporary Stress in the Southern Flank of Central Alborz. International Institute of Earthquake Engineering and Seismology, Tehran, Iran, p. 122. Publication No: 81-2003-7 (in Persian).

Alavi, M., 1996. Tectonostratigraphic synthesis and structural style of the Alborz mountain system in northern Iran. Journal of Geodynamics 21, 1–33.

Allen, M.B., Vincent, S.J., Alsop, I., Ismail-zadeh, A., Flecker, R., 2003a. Late Cenozoic deformation in the South Caspian region: effects of a rigid basement block within a collision zone. Tectonophysics 366, 223–239.

Allen, M.B., Ghassemi, M.R., Shahrabi, M., Qorashi, M., 2003b. Accommodation of late Cenozoic oblique shortening in the Alborz range, northern Iran. Journal of Structural Geology 25, 659–672.
Allenbach, P., 1966. Geologie und petrographie des Damavand und seiner Umgebung (Zentral Elburz): Iran. Geol. Mitt. Geol. Inst. ETH Univ. Zurich, n. s., 63, p. 144 (in German).
Ambraseys, N.N., Melville, C.P., 1982. A History of Persian Earthquakes. Cambridge University Press, New York.
Ashtari, M., Hatzfeld, D., Kamalian, M., 2005. Microseismicity in the region of Tehran. Tectonophysics 395, 193–208.
Axen, G.J., Lam, P.J., Grove, M., Stockli, D.F., Hassanzadeh, J., 2001. Exhumation of the west-central Alborz mountains, Iran, Caspian subsidence, and collision-related tectonics. Geology 29, 559–562. doi:10.1130/0091-7613(2001) 029<0559:EOTWCA>2.0.CO;2.
Bachmanov, D.M., Trifonov, V.G., Hessami, Kh.T., Kozhurin, A.I., Ivanova, T.P., Rogozhi, E.A., Hademi, M.C., Jamali, F.H., 2004. Active faults in the Zagros and central Iran. Tectonophysics 380, 221–241.
Ballato, P., Nowaczyk, N.R., Landgraf, A., Strecker, M.R., Friedrich, A., Tabatabaei, S.H., 2008. Tectonic control on sedimentary facies pattern and sediment accumulation rates in the Miocene foreland basin of the southern Alborz mountains, northern Iran. Tectonics 27, TC6001. doi:10.1029/2008TC002278 (3.413).
Berberian, M., 1976. Contribution on the Seismotectonics of Iran: Part I. Geological Survey of Iran, Tehran. 517 pp.
Berberian, M., 1983. The southern Caspian: a compressional depression floored by a trapped, modified oceanic crust. Canadian Journal of Earth Sciences 20, 163–183.
Berberian, M., 1994. Natural Hazards and the First Earthquake catalogue of Iran, vol. 1, Historical Hazards in Iran Prior to 1900, A UNESCO/IIEES Publication during UN/IDND International Institute of Earthquake Engineering and Seismology Tehran, 603 + 66 p.
Berberian, M., King, G.C.P., 1981. Towards a paleogeography and tectonic evolution of Iran. Canadian Journal of Earth Sciences 18, 210–265.
Berberian, M., Yeats, R.S., 1999. Patterns of historical earthquake rupture in the Iranian plateau. Bulletin of the Seismological Society of America 89, 120–139.
Berberian, M., Yeats, R.S., 2001. Contribution of archaeological data to studies of earthquake history in the Iranian plateau. Journal of Structural Geology 23, 563–584.
Berberian, M., Qorashi, M., Arzhang-ravesh, B., Mohajer-Ashjai, A., 1985. Recent Tectonics, Seismotectonics and Earthquake Fault Hazard Investigations in the Greater Tehran Region: Contribution to the Seismotectonics of Iran: Part V: Geological Survey of Iran, report 56, p. 316.
Breddin, H., 1970. Der Elburz im Iran, ein Schuppengebirge. Geological Mitting (Aachen) 10 (196) 1, 61-100 (in German).
Dellenbach, J., 1964. Contribution à l'étude géologique de la région située à l'est de Téhéran (Iran). Faculté des Science de l'Universite Strasbourg (France), 117 pp. (in French).
Djamour, Y., 2004. Contribution de la Géodésie (GPS et nivellement) à l'étude de la déformation tectonique et de l'aléa seismique sur la région de Téhéran (montagne de l'Alborz, Iran). Faculté des Sciences et des techniques du Languedoc l'Université Montpellier II (France). . 180 pp. (in French).
Djamour, Y., Bayer, R., Vernant, P., Hatam, Y., Ritz, J.F., Hinderer, J., Luck, B., Nankali, H., Le Moigne, N., Sedighi, M., Boy, J.P., 2008. The Present-day Deformation in Alborz (Iran) Depicted by GPS and Absolute Gravity Observations: Paris, France, SGF.
Dresch, J., 1961. Le piedmont de Téhéran, Les observations de géographie physique en Iran septentrional: Centre Documentation Cartographique et géographique, Mémoires et Documents, 8, pp. 85–101 (in French).
Geological Survey of Iran, 1993. 1:100,000 Geology Map of Tehran. Geological Survey of Iran, Tehran.
Guest, B., Axen, G.J., Lam, P.S., Hassanzadeh, J., 2006. Late Cenozoic shortening in the west central Alborz mountains, northern Iran, by combined conjugate strike–slip and thin-skinned deformation. Geosphere 2, 35–52. doi:10.1130/GES00019.1.
Hedayati, A., Brander, J.L., Berberian, M., 1976. Microearthquake survey of Tehran region. Iran. Bulletin of the Seismological Society of America 66, 1713–1725.
Hessami, K., Jamali, F., Tabassi, H., 2003. The Map of Major Active Faults of Iran. International Institute of Earthquake Engineering and Seismology.
Hollingsworth, J., 2007. Active Tectonics of NE Iran, PhD thesis University of Cambridge, 220 p.
Hollingsworth, J., Jackson, J., Walker, R., Nazari, H., 2008. Extrusion tectonics and subduction in the eastern South Caspian. Journal of Geology 36 N. 10, 763–766.
Jackson, J., Priestley, K., Allen, M., Berberian, M., 2002. Activetectonics of the South Caspian Basin. Geophysical Journal International 148, 214–245.
Knill, J.L., Jones, K.S., 1968. Ground water conditions in Greater Tehran. Quarterly Journal of Engineering Geology and Hydrogeology 1, 181–194.
Landgraf, A., Ballato, P., Strecker, M.R., Friedrich, A., Tabatabaei, S.H., Shahpasandzadeh, M., 2009. Fault-kinematic and geomorphic observations along the North Tehran Thrust and Mosha Fasham Fault, Alborz mountains Iran: implications for fault-system evolution and interaction in a changing tectonic regime. Geophysical Journal International 177, 676–690.
Moinabadi, M.E., Yassaghi, A., 2007. Geometry and kinematics of the Mosha fault, south Central Alborz Range, Iran: an example of basement involved thrusting. Journal of Asian Earth Science 29, 928–938.
Nabavi, M.H., 1976. Preface to Geology of Iran. Geological survey of Iran. 109 pp.
Nazari, H., 2006. Analyse de la tectonique récente et active dans l'Alborz Central et la région de Téhéran: Approche morphotectonique et paléoseismologique. Faculté des Sciences et des techniques du Languedoc l' Université Montpellier II (France). 246 pp. (in French).
Nazari, H., Ritz, J.F., Shafei, A., Ghassemi, A., Salamati, R., Michelot, J.L., Massault, M., 2009. Morphological and paleoseismological analyses of the Taleghan fault, Alborz, Iran. Geophysical Journal International 178, 1028–1041.
Negahban, E.O., 1977. Report of Preliminary excavations at Tapeh Sagzabadin the Qazvin plain. Marlik. Journal of the Institute and Department of Archaeology 2, Faculty of Letters and Humanities, Tehran University, 26 and 45 p. (in Persian and English).
Pedrami, M., 1983. Plio-Pleistocene in Iran. Geological survey of Iran. 10 pp.
Rieben, E.H., 1955. The geology of Tehran plain. American Journal of Science 253, 617–639.
Ritz, J.F., 2009. Extrusion tectonics and subduction in the eastern South Caspian region since 10 Ma: Comment, Geology 37, E191-E191.
Ritz, J.F., Balescu, S., Soleymani, S., Abbassi, M.R., Nazari, H., Feghhi, K., Shabanian, E., Tabassi, H., Farbod, Y., Lamothe, M., Michelot, J.L., Massault, M., Che'ry, J., Vernant, P., 2003. Determining the Long-term Slip Rate Along the Mosha Fault, Central Alborz, Iran: Implications in Terms of Seismic Activity, S.E.E. 4 Meeting, Tehran, 12–14 May.
Ritz, J.F., Nazari, H., Salamati, R., Shafeii, A., Solaymani, S., Vernant, P., 2006. Active transtension inside Central Alborz: a new insight into the Northern Iran–Southern Caspian geodynamics. Geology 34, 477–480.
Sieber, N., 1970. Zur geologie des gebietes sudlich des Taleghan-tales, Zentral Elburz (Iran): Europaische Hochsch, Schrschriften, 19(2, p. 126 (in German).
Solaymani, Sh., Feghhi, Kh., Shabanian, E., Abbassi, M.R., Ritz, J.F., 2003. Preliminary Paleoseismological Studies on the Mosha Fault at Mosha Valley. International Institute of Earthquake Engineering and Seismology. . 89 pp. (in Persian).
SRTM data website; http/:edcsgs9.cr.usgs.gov/pub/data/srtm/.
Steiger, R., 1966. Die geologie der west-Firuzkuh area (Zentral Elburz/Iran). Mitteilung Geologisches Institut, ETH-Zurich. 145 pp. (in German).
Stöcklin, J., 1968. Structural history and tectonics of Iran. A review. Bulletin of American Association of Petroleum Geology 52 (7), 1229–1258.
Stöcklin, J., 1974. Northern Iran: Alborz Mountains. In: Spencer, A.M. (Ed.), Mesozoic–Cenozoic Belts: Geological Society of London, Special Publications, 4, pp. 213–234.
Talai, H., 1998. Preliminary report of the 10th excavation season (1998) at Tappeh Sagzabad, Qazvin Plain. Archaeological Institute, Tehran University, unpublished internal report, 31 p.
Tatar, M., Hatzfeld, D., 2009. Microseismic evidence of slip partitioning for the Rudbar-Tarom earthquake (*Ms* 7.7) of 1990 June 20 in NW Iran. Geophisical Journal International 176, 529–541.
Tchalenko, J.S., Berberian, M., Iranmanesh, H., Bailly, M., Arsovsky, M., 1974. Tectonic framework of the Tehran region, Geological Survey of Iran, Report n° 29.
Tchalenko, J.S., 1975. Seismotectonics framework of the North Tehran fault. Tectonophysics 29, 411–420.
Trifonov, V.G., Hessami, K.T., Jamali, F., 1996. West-Trending Oblique Sinitral—Reverse Fault system in Northern Iran: IIEES Special Publication 75. Tehran, Iran.
Vernant, P., Nilforoushan, F., Che'ry, J., Bayer, R., Djamour, Y., Masson, F., Nankali, H., Ritz, J.F., Sedighi, M., Tavakoli, F., 2004. Deciphering oblique shortening of central Alborz in Iran using geodetic data. Earth and Planetary Science Letters 223, 177–185.
Zanchi, A., Berra, F., Mattei, M., Ghassemi, M.R., Sabouri, J., 2006. Inversion tectonics in central Alborz, Iran. Journal of Structural Geology 20, 1–15.